

PAPER • OPEN ACCESS

## Experimental study on creep-ageing anisotropy behavior of 2195 Al-Cu-Li alloy

To cite this article: G P Li *et al* 2020 *J. Phys.: Conf. Ser.* **1681** 012005

View the [article online](#) for updates and enhancements.

You may also like

- [Concluding Remarks](#)  
R C Thompson
- [The 22nd EGAS Conference of the European Group for Atomic Spectroscopy](#)  
A Arnesen and R Hallin
- [Relativistic Many-Body Calculations](#)  
I Lindgren



**ECS**  
The  
Electrochemical  
Society  
Advancing solid state &  
electrochemical science & technology

**DISCOVER**  
how sustainability  
intersects with  
electrochemistry & solid  
state science research

# Experimental study on creep-ageing anisotropy behavior of 2195 Al-Cu-Li alloy

G P Li<sup>1</sup>, L H Zhan<sup>1,2,a</sup>, Y L Yang<sup>1</sup> and X Wang<sup>1</sup>

<sup>1</sup> College of Mechanical and Electrical Engineering, Central South University, Changsha 410083, PR China

<sup>2</sup> State Key Laboratory of High-Performance Complex Manufacturing, Central South University, Changsha 410083, PR China

<sup>a</sup> E-mail: 2445031536@qq.com

**Abstract.** The problem of anisotropy in Al-Cu-Li alloy leading to low precision of formed component becomes one of important obstacles to accurately predict creep aging forming (CAF). In-planer anisotropy in creep-ageing behavior of a textured 2195-T34 alloy was investigated in this paper. The total creep deformation in the rolling direction is much smaller than that in the other directions. The tensile strength and yield strength of specimens in all directions are similarly enhanced during creep aging, indicating that the precipitation was relatively uniform in different directions. The EBSD results show that the strong texture is the main reason for the uneven strength with different angles. A constitutive model describing creep-ageing anisotropy was established and the optimal parameters of the equation were obtained by optimization algorithm. The creep strain of all angles predicted by the equation is in good agreement with the experimental results. The proposed constitutive modeling can be applied to accurately simulate the CAF of 2195-T34 alloy structural parts.

## 1. Introduction

Creep age forming (CAF) is a new sheet metal forming technology, which consists of creep and age hardening. In this process, the workpiece is loaded onto a mold with vacuum bagging or mechanical clamping, then heated to a certain temperature and kept for a controlled amount of time; at last, the elastic deformation is in part transformed into plastic deformation, and the strength of the alloy is improved. This technology shows wide application in aviation and aerospace industry, such as B-1B long range combat aircraft, the upper wing skins of the Gulfstream GIV and Airbus A330/340/380 [1]. Al-Cu-Li alloys have shown wide application in recent years due to their excellent performance, including low density, high elastic modulus, high specific rigidity, high specific strength, sound fatigue resistance, good weldability and corrosion resistance [2]. Although the addition of lithium to the Al-Cu alloy can improve the mechanical properties of the material, it brings a strong texture and causes a negative impact on forming and strengthening. Some researchers have studied the effect of texture on properties, and found that Brass texture causes strong anisotropy through weakening the performance at 45 °direction [3].

The application of CAF technique to Al-Cu-Li alloys is a matter of concern to many scholars. Hu et al. [4] showed that applied stress during aging of 2195 aluminum alloy can increase peak strength and promote T1 phase to precipitate. Zhang et al. [5] studied the effect of pre-stretching on the creep aging process of Al-Cu-Li alloy. The introduction of proper pre-stretching can significantly increase creep strain and yield strength, but excessive pre-deformation suppresses creep strain and the alloy strengthening effect is obviously reduced. Li et al. [6] investigated the creep ageing behavior of Al-



Cu-Li alloy under tensile and compressive stresses. Their predicted springback results of CAF of thin plates considering both tensile and compressive stress is consistent with the experimental values. However, the anisotropy in creep behavior of Al-Cu-Li alloy has not been reported yet.

The aim of this paper is to investigate the in-plane creep anisotropy behavior of 2195T34 alloy. The electron back-scattered diffraction (EBSD) was performed to observe the texture in the as-received plate. The mechanical property anisotropy was studied by tensile test and the calculation of Schmidt factor, and the creep ageing behavior at 0 °, 45 °, and 90 ° to the rolling direction were examined. Additionally, a constitutive equation describing creep anisotropy was established based on the Hill equivalent stress and Kowalewski damage model.

## 2. Experimental Procedures

The material used in this work was a hot-rolled 2195 alloy plate of 8.5 mm in thickness and the chemical compositions is listed in Table 1. The as-received plate was subjected to solution treatment at 510 °C for 30 minutes followed by water quenching at room temperature. 4% compression deformation along the rolling direction was applied to the solution treated plate. Bone-shaped samples (fig 1.) with a gauge length of 35 mm and a diameter of 5 mm were machined in the plane at 0 °, 45 °, and 90 ° to the rolling direction after the plate was fully natural-aged for two weeks at room temperature.

**Table 1.** Main chemical compositions of AA 2195 (wt%).

Cu	Li	Mg	Zr	Ag	Fe	Si	Ti	Mg	Al
4.05	0.99	0.31	0.15	0.27	0.051	<0.062	<0.03	<0.018	balance

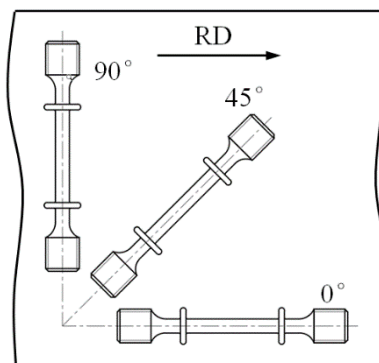


**Fig 1.** Samples for creep aging test.

The slice along the transverse plane of 4% pre-deformed plate is cut for EBSD test, and its upper surface is mechanically polished. The sections were electropolished using 30 vol.% HNO<sub>3</sub> acids in methanol followed by examined and analyzed using HKL Channel 5 software in a FEI Helios Nanolab 600i system at a sample tilt of 70° with an accelerating voltage of 20 kV. Step size was 1 μm, and the number of data points is 250×350.

Creep ageing tests were conducted on a RMT-D5 Creep Test Machine with an assisting furnace. The temperature was raised to 180 °C at the heating rate of 5 °C/min and kept for 10 min, then a stress of 160MPa was applied to the samples and hold for 20 hours. The creep strain was obtained from the computer after test. Tensile tests were completed in a MTS-E45 universal testing machine at a crosshead speed of 2 mm/min at room temperature and repeated three times for each condition.

## 3. Results and discussion

### 3.1. Texture of the initial materials

Due to the presence of lithium, the microstructure usually shows a strong orientation, which is closely related to the anisotropic behavior of the material. The orientation distribution functions (ODFs) section ( $\phi_2 = 0^\circ, 45^\circ$  and  $65^\circ$ ) of 2195-T34 aluminum alloy in transverse direction is presented in Fig. 2. The ODFs section exhibits typical rolling textures including dominant  $\{110\} \langle 112 \rangle$  brass and  $\{123\} \langle 634 \rangle$  S texture, and observed weak  $\{112\} \langle 111 \rangle$  copper and  $\{100\} \langle 001 \rangle$  cube. It is generally believed that the strong texture caused by the introduction of lithium is the main reason for the anisotropy of the mechanical properties of the Al-Li alloys [7, 8]. Table 2. shows the maximum Schmid factor (MSF) of each grain under different stress directions calculated by HKL Channel 5 software, and the average value is given. Details regarding Schmid factor calculation can be found from the references [9]. The average of MSF is 0.406, 0.457 and 0.415 when the angle between the applied stress and the rolling direction is  $0^\circ, 45^\circ$  and  $90^\circ$ , respectively. Generally, the hardness of the grain is inversely related to the Schmidt factor. Therefore, the overall strength of 2195 alloy is largest at the  $0^\circ$  orientation and smallest at the  $45^\circ$  orientation.

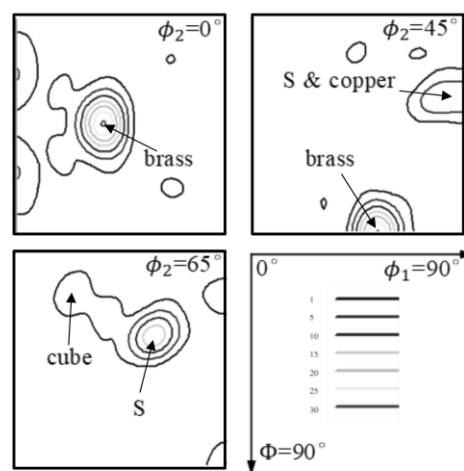


**Fig 2.** ODF section of 2195 Al-Cu-Li alloy.

**Table 2.** The maximum Schmid factor of the 2195 alloy sample in different angles of  $0^\circ, 45^\circ$  and  $90^\circ$  between tensile stress direction and rolling direction.

Orientations	Thr maximum Schmid factor
$0^\circ$	Roman type
$45^\circ$	Bold type
$90^\circ$	Roman type

### 3.2. Mechanical properties

Table 3 shows the mechanical properties of 2195 aluminum alloy before and after creep aging. the strength of the material increases and the elongation decreases after aging, which is mainly attributed to the strengthening effect of the precipitate. For all samples in different aging times, the yield strength and tensile strength is the largest in the rolling direction and the smallest in the  $45^\circ$  direction, which is consistent with the Schmid factor calculation results. It is worth noting that the aging enhancement effect is basically the same for samples in all directions, with the approximately increase of 190 MPa for yield strength and 105 MPa for tensile strength. According to the above results, it can be concluded that the precipitations have similar strengthening effect for all direction specimens during creep aging and the strength increased during creep aging is not affected by texture.

**Table 3.** the mechanical properties of 2195 aluminum alloy in different aging time.

Aging time (h)	Orientations	Yield strength (MPa)	Tensile strength (MPa)	Elongation (%)
0h	0 °	381	501	12.2
	45 °	321	415	20.9
	90 °	362	480	17.6
20h	0 °	570	604	7.2
	45 °	512	529	11.9
	90 °	556	588	8.5

### 3.3. Creep ageing behavior under the loads in different directions

The creep aging behavior of 2195 alloy in different directions of 0°, 45° and 90° under 160MPa tensile stress at 180 °C for 20h are presented in Fig 3. The experimental data was recorded 10 minutes after loading, in order to avoid data errors caused by early temperature unevenness. These creep curves show similar trend during the test time in Fig 3(a). It is observed that all creep curves are divided into two stages, named primary creep and steady-state respectively. The creep strain increases sharply with time at the beginning of creep test and tends to equilibrium stage with decreasing creep rate, which is attributed to the interaction between movements of dislocation and precipitates formed in the matrix. Usually the creep mechanism is different in different creep stages [10].

It is found from the Fig 3(a) that the total creep deformation increases with angle relative to rolling direction. The creep strain in the 0° direction is much smaller than the other two. As seen from Fig 3(b), it can be found that the creep rate difference is obvious in the early stage, which decreases continuously as the creep aging progresses, and finally disappears after 4.5 hours. The creep strain difference between the 0° and 90° samples reaches a maximum of 0.059% at this time, and remains the same until the end of the experiment. Taking 4.5 hours as the boundary, the creep curves are artificially divided into a creep anisotropy increase (CAI) stage and a creep anisotropy maintenance (CAM) stage. The CAI phase and the CAM phase are highly coincident with primary creep and steady-state creep. It implies that the change of creep mechanism causes the change of creep anisotropic behavior. It is noteworthy that the anisotropy of creep behavior does not match the anisotropy of mechanical properties, and the mechanism of creep anisotropy in 2195 alloy needs further study.

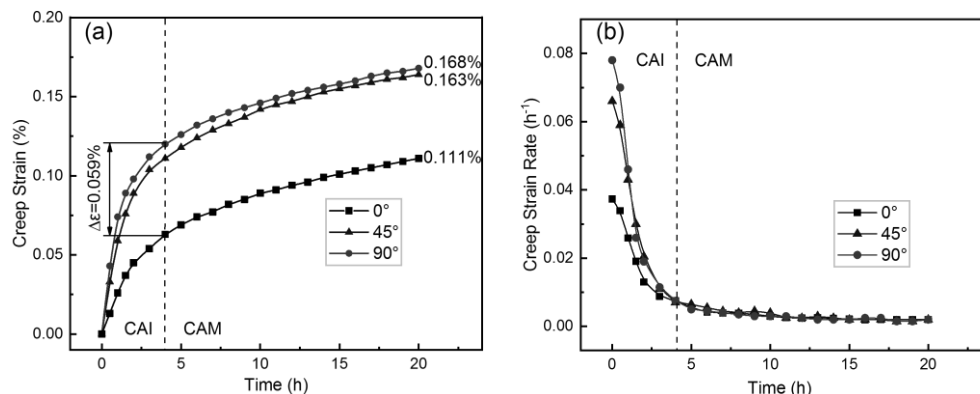


**Fig 3.** creep deformation in 0°, 45° and 90° at the creep temperatures of 180 °C under 160 MPa: (a) creep strain curves; (b) creep strain rate curves.

### 3.4. Creep model considering anisotropy

A two-stage creep strain rate equation with hyperbolic function under uniaxial stress, which is adapted from Kowalewski's model [11], is written as following:

$$\dot{\epsilon} = A \cdot \sinh[B \cdot \sigma \cdot (1 - H)] \quad (1)$$

$$\dot{H} = \frac{h}{\sigma} \left(1 - \frac{H}{H^*}\right) \cdot \dot{\epsilon} \quad (2)$$

Where  $\dot{\epsilon}$  is creep rate and  $\sigma$  is uniaxial stress in Eq. (1), the variable  $H$  varies from 0 at the beginning of the creep process to  $H^*$  in Eq. (2), which is used to indicate the attenuation of creep rate.  $A$ ,  $B$ ,  $H^*$  are constants in the function.

In general, the nature of creep is anisotropic, and the isotropic phenomenon of material creep can be treated as a special case of the anisotropy. Since it is difficult to directly construct the anisotropic creep model due to the complexity of anisotropic, the isotropic models are extended to models considering the creep anisotropy [12]. Based on the simplified isotropic creep constitutive model, a new creep anisotropy model can be developed by introducing the Hill's equivalent stress in this paper.

$$\sigma_{hill} = \sqrt{F \cdot \sigma_{11}^2 + G \cdot \sigma_{22}^2 - 2M\sigma_{11} \cdot \sigma_{22} + 2N\sigma_{12}^2} \quad (3)$$

$$\dot{\epsilon} = A \cdot \sinh[B \cdot \sigma_{hill} \cdot (1 - H)] \quad (4)$$

$$\dot{H} = \frac{h}{\sigma^m} \left(1 - \frac{H}{H^*}\right) \cdot \dot{\epsilon} \quad (5)$$

In Eq. (3) and Eq. (4),  $\sigma_{hill}$  is Hill's equivalent stress in plane,  $F$ ,  $G$ ,  $M$ , and  $N$  represent anisotropic parameters.  $\sigma_{11}$ ,  $\sigma_{22}$  and  $\sigma_{12}$  are Cauchy stress tensors. All constants can be determined by the least squares evaluation.

Fig 4 shows the comparison of the computed creep strain and experimental data in different directions to the rolling direction. The results show that the curves fitted by the new model are in good agreement with the general trend of the actual experimental values, which confirms that the established model can effectively predict the creep anisotropy of 2195 aluminum alloy. The material constants for 2195 Al-Cu-Li alloy are listed in Table 4.

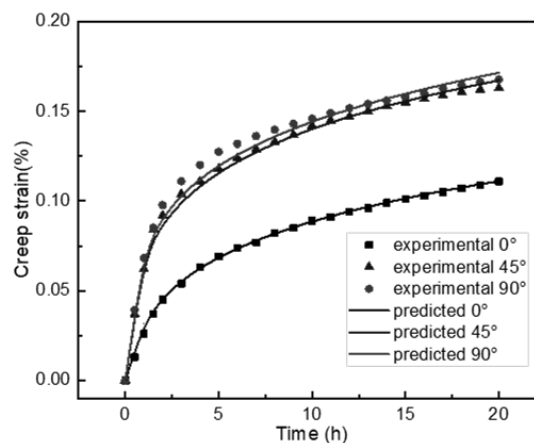


**Fig 4.** Comparisons of the measured and predicted creep strains of 2195 alloy in different directions at the creep temperatures of 180°C under 160 MPa.

**Table 4.** Material constants in creep anisotropy model for 2195 aluminum alloy at 180 °C.

$A$	$B$	$h$	$H^*$	$m$	$F$	$G$	$M$	$N$
2.170	$1.374 \times 10^{-4}$	$3.988 \times 10^{10}$	0.966	3.527	1.02	1.707	1.153	3.043

#### 4. Conclusions

The creep ageing anisotropy behavior in 2195 Al-Cu-Li alloy are experimentally studied by creep tests, tensile strength tests and EBSD tests. The main findings can be summarized as follows: ch figure should have a brief caption describing it and, if necessary, a key to interpret the various lines and symbols on the figure.

a) The mechanical property test shows strong anisotropy. The strength is the highest in the rolling direction and the weakest in the direction of  $45^\circ$ , and this difference is not affected by aging enhancement. Based on the average maximum Schmid factor analysis, strong brass texture and S texture is the main reason for the anisotropy of the mechanical properties of 2195 alloy.

b) The creep strain for 2195 Al-Cu-Li alloy in rolling direction is obviously smaller than that in  $45^\circ$  and  $90^\circ$  directions. This difference arises from the primary creep stage and remains unchanged during the steady-state creep stage.

c) An anisotropy creep model is established, which can accurately describe the creep ageing behavior of the 2195 alloy in different directions at ageing temperature. By introducing Hill's equivalent stress tensor, the anisotropy creep model can be easily complied into the simulation software.

#### References

- [1] Ho K C, Lin J and Dean T A 2004 Constitutive modelling of primary creep for age forming an aluminium alloy *J MATER PROCESS TECH*, **153-154** pp 122-127
- [2] Honma T, Yanagita S, Hono K, Nagai Y, Hasegawa M, Coincidence Doppler broadening and 3DAP study of the pre-precipitation stage of an Al-Li-Cu-Mg-Ag alloy *ACTA MATER*, **52** pp 1997-2003
- [3] El-Aty A A, Xu Y, Zhang S H, Ma Y and Chen D Y 2017 Experimental investigation of tensile properties and anisotropy of 1420, 8090 and 2060 Al-Li alloys sheet undergoing different strain rates and fibre orientation: a comparative study *Procedia Engineering* **207** pp 13-18
- [4] Hu L B, Zhan L H, Shen R L, Liu Z, Ma Z, Liu J and Yang Y 2017 Effects of uniaxial creep ageing on the mechanical properties and micro precipitates of Al-Li-S4 alloy *Materials Science and Engineering: A* **688** pp 272-279
- [5] Zhang J, Li Z D, Xu F S and Huang C 2019 Regulating effect of pre-stretching degree on the creep aging process of Al-Cu-Li alloy *Materials Science and Engineering: A* **763** 138157
- [6] Li Y, Shi Z S, Lin J G, Yang Y L, Rong Q, Huang B M, Chung T, Tsao T, Yang J and Balint D S 2017 A unified constitutive model for asymmetric tension and compression creep-ageing behaviour of naturally aged Al-Cu-Li alloy *INT J PLASTICITY* **89** pp 130-149
- [7] Nayan N, Mishra S, Prakash A, Sarkar R, Murty S V S N, Yadava M, Prasad M J N V and Samajdar I 2018 Origin of through-thickness serrated tensile flow behavior in Al-Cu-Li (AA2195) alloy: Effect of microstructure and texture *Materialia* **5** 100180
- [8] Fan W, Kashyap B P and Chaturvedi M C 2003 Anisotropy in flow and microstructural evolution during superplastic deformation of a layered-microstructured AA8090 Al-Li alloy *Materials Science and Engineering: A* **349** pp 166-182
- [9] Xia D B, Chen S, Huang G S, Jiang B, Tang A T, Yang H, Gavras S, Huang Y D, Hort N and Pan F 2019 Calculation of Schmid factor in Mg alloys: Influence of stress state, *SCRIPTA MATER*, **171** pp 31-35
- [10] Yang Y L, Zhan L H, Ma Q Q, Feng J W and Li X C 2016 Effect of pre-deformation on creep age forming of AA2219 plate: Springback, microstructures and mechanical properties, *J MATER PROCESS TECH* **229** pp 697-702
- [11] Kowalewski Z L, Hayhurst D R and Dyson B F 1994 Mechanisms-based creep constitutive equations for an aluminium alloy *Journal of Strain Analysis for Engineering Design* **29 no 4** pp 309-316
- [12] Meng Q H and Wang Z Q 2019 Creep damage models and their applications for crack growth analysis in pipes: A review *Engineering Fracture Mechanics* **205** pp 547-576